RESONANCE IN RANDOM π-NETWORK POLYMERS*

D.J. KLEIN, T.P. ŽIVKOVIĆ* and N. TRINAJSTIĆ*

Department of Marine Sciences, Texas A&M University at Galveston, Galveston, Texas 77553, USA

Received 8 September 1986
(in final form 18 March 1987)

Abstract

The electronic structure of a π-network polymer with random numbers of two types of monomer units is considered in a "conjugated circuit" resonance-theoretic framework. A transfer-matrix technique for computing relevant ensemble-average energies is described and applied to a few example simple benzenoid systems. A type of long-range ordering is noted to be relevant, and some of its implications are discussed.

1. Introduction

Recently, there has been much interest [1–4] in π-network polymers and their electronic structure. In both physics and chemistry, the relevant polymer structures have been viewed to be regular, i.e. translationally symmetric. However, polymerization processes typically proceed with varying amounts of impurities of defects. Indeed, the standard phrase [5] "copolymerization" applies to the oft-encountered regime with a high concentration of two types of monomer units. Here, we investigate the effects of a random admixture of two types of monomer units upon the electronic structure of π-network polymers where, because of π-electron "delocalization", one might expect that "long-range" effects of the disorder are most pronounced. In allowing the possibility of such qualitative effects, we focus on the limit of very long polymer chains.

Although there has been much previous work [6] on the effects of disorder upon electronic structure, our present study differs in a couple of qualitative ways. First, our monomer units are generally more complex than the usual single site.

*Research supported by the Robert A. Welch Foundation of Houston, Texas, USA.
*Permanent address: The Rugjer Bošković Institute, P.O. Box 1016, 41001 Zagreb, Croatia, Yugoslavia.

Second, rather than the usual molecular-orbital (or tight-binding band-theoretic) approaches, we take a valence-bond resonance-theoretic approach involving Kekulé structures, as outlined in sect. 2. The "transfer-matrix" computational method described in sects. 3, 4 and 6 is an extension of that which we have previously used [7,8] on regular chains or strips. Section 5 concerns "boundary conditions" at the strip ends, which turns out to be of some use in sects. 6–9. Questions of asymptotic behavior of averages for different ensembles are addressed in sects. 7 and 8, and some of these questions are answered. Section 9 directs attention to a type of long-range order involving different π-bonding patterns. The possibility of phase transitions between phases of different long-range orders is noted. Section 10 summarizes the relevant computations in applications. Sections 11–14 illustrate the application to four example systems, at least one of which exhibits a transition between two different phases.

2. Problem formulation

For the π-network polymer studied here, a simple resonance-theoretic model is used, namely the *conjugated-circuit* model. This model may be motivated from an empirical point of view [9] elaborating Clar's ideas, or from a more quantum-chemically motivated view [10]. Either approach leads [11] to simply stated subgraph-enumeration problems. The first problem for a π-network with graph G is that of finding the number $K(G)$ of its *Kekulé structures*. Each such structure may be viewed as a union or superposition of G and a unique corresponding *1-factor*, a 1-factor of G being a spanning subgraph every factor of which has degree 1. Given a 1-factor and an (even) length-m cycle of G, this cycle is said to identify a *conjugated m-circuit* of the associated Kekulé structure iff alternate edges of this cycle occur in the 1-factor. The second type of problem of interest is to find the sum $\#^{(m)}(G)$ over all Kekulé structures of the numbers of conjugated m-circuits in each structure. Then an estimate of the total π-electron resonance energy for the molecule G is [9, 11]

$$E(G) = \sum_p \{R_p \#^{(4p+2)}(G) + Q_p \#^{(4p)}(G)\}/K(G),$$

where R_p and Q_p are parameters.

For the polymer problem here, we seek for various properties associated averages or, more generally, weighted sums, over a relevant ensemble of systems G. The members of such an ensemble will have a given number L of monomers, attention here being restricted for the most part to just two types of monomer units, say A and B, at any position along a polymer chain. An average Kekulé structure count over all chains with a and $b = L - a$ units of types A and B, respectively, is

$$K_{a,b} \equiv \binom{a+b}{a}^{-1} \sum_{G}^{a,b} K(G), \tag{2.1}$$

the binomial coefficient simply being the number of terms occurring in the sum. A weighted sum over various choices of a and b is defined as

$$K_L \equiv K_L(x,y) \equiv \sum_{G}^{L} K(G)\, x^{a(G)}\, y^{b(G)}, \tag{2.2}$$

where $a(G)$ and $b(G)$ are the numbers of A and B monomer units in G, and the sum is over all systems of length L. Mathematically, x and y are variables in a *generating function*, with $\binom{a+b}{a} K_{a,b}$ being the coefficient of $x^a y^b$. In a more physico-chemical vein, we view x and y as *activities*, for A and B monomers. The function of (2.2) is clearly converted to a (weighted) average upon division by

$$\sum_{G}^{L} x^{a(G)} y^{b(G)} = (x+y)^L, \tag{2.3}$$

this average being independent of a rescaling of both x and y. Then, we will ultimately choose

$$x + y = 1, \tag{2.4}$$

whence (2.2) itself becomes the (sought-after) average.

In addition to the Kekulé structure counts $K_{a,b}$ and K_L, conjugated-circuit counts and energies are defined in exact parallel. The estimation of the overall energies averaged over either ensemble is to be made in terms of these various counts, as described in sect. 8.

There are crucial chemical assumptions involved in identifying the particular ensembles as in (2.1) and (2.2) as being those of experimental relevance. Indeed, the "proper" choice of ensemble relates to the mechanism of chain formation if we allow for the possibility that the orderings of monomer units that result can be *quenched in* (i.e. with no relaxation after being grown). For the ensemble of (2.2), one consistent growth process is that where A and B monomers would slowly and randomly impinge (with some relative frequencies) upon the growing chain end, such that whatever hits the chain end sticks upon contact. More general ensembles can be imagined wherein A and B monomers attach during growth with different probabilities to different types of chain ends. Then an ensemble with additional activity weightings arises: for instance, u, v and w to be raised to powers $aa(G)$, $ab(G) = ba(G)$ and $bb(G)$, being numbers of nearest-neighbor AA, AB and BB monomer pairs in

a polymer graph G. Although such ensemble averages often are treatable via the same type of transfer-matrix approach discussed in the following, we presently restrict attention to the simpler cases of (2.1) and (2.2).

3. Transfer matrix approach

The various desired enumerations are to be carried out via transfer matrix [7,8,12]. There are basic transfer matrices for each type of monomer unit. To construct these, imagine a general polymer chain divided into various monomer cells with the cell boundaries intersecting bonds rather than sites. For example, in fig. 1 such

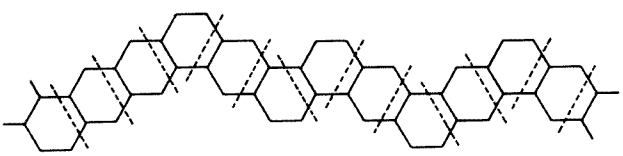

Fig. 1. Portion of a polyphene polymer with random straight-ahead (anthracenoid) and bent (phenanthrenoid) linkages. The dashed lines indicate divisions between monomer cells.

cell boundaries are indicated by dashed lines. The σ-bonds cut through on a boundary can be "occupied" in different manners in various 1-factors. If there are P bonds that are cut, then generally there will be as many as 2^P ways of occupying them in a 1-factor. Each such manner of occupation is a *local state* $|\xi)$, designatable by a sequence of P binary digits (1 and 0) to indicate which are occupied and which are unoccupied. The four types of local states, and their binary designations, which arise

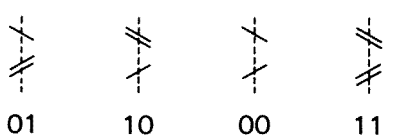

Fig. 2. Local (bond-occupancy) states for the edges intersected by the dashed cell-boundary lines of fig. 1.

in conjunction with the system of fig. 1 are indicated in fig. 2. Next, we let $(\zeta|T_A|\xi)$ be the number of 1-factors that can occur within a single A-type monomer cell if the first side of the cell is constrained to have local state $|\xi)$ and the succeeding side along the polymer chain is constrained to have local state $|\zeta)$. The array of these numbers is the *transfer matrix* T_A, and T_B is defined similarly. The trace of an L-fold product of transfer matrices is then of the form

$$\mathrm{tr}\left\{\prod_{i=1}^{L} T_{C_i}\right\} = \sum_{\xi_1,\ldots,\xi_L} \prod_{i=1}^{L} (\xi_i | T_{C_i} | \xi_{i-1}), \tag{3.1}$$

where $\xi_0 \equiv \xi_{L+1}$ and the C_i are A or B. However, each product on the right-hand side is seen to give the number of Kekulé structures in a cyclic polymer chain with local states $\xi_1, \xi_2, \ldots, \xi_L$ located at the positions $1, 2, \ldots, L$. Consequently, the total trace of (3.1) counts the total number of Kekulé structures $K(G)$ in a polymer G identified to the sequence of monomers C_i. Then a weighted summation over all possible such sequences would lead to K_L; this weighted sum can be expressed as

$$K_L = \mathrm{tr}\,(x\,T_A + y\,T_B)^L = \mathrm{tr}\,\mathcal{T}^L, \quad \text{cyclic chains}, \tag{3.2}$$

where we have introduced an *ensemble transfer matrix*

$$\mathcal{T} \equiv x\,T_A + y\,T_B\,. \tag{3.3}$$

If K_L is obtained as a polynomial in x and y, then $K_{a,b}$ can be recovered from the coefficient of $x^a y^b$.

As an example, consider the case of fig. 1, where each cell is seen to involve either a straight-chain "anthracene" (A) linkage or a bent "phenanthrene" (B) linkage. For an A-type cell there are just five local Kekulé structures within a monomer cell,

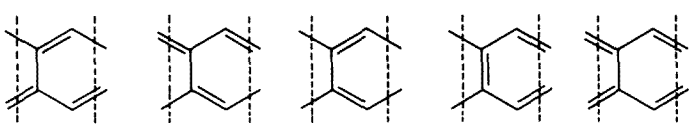

Fig. 3. Manners of "growth" of Kekulé structures from one local state (on the left) across an anthracenoid linkage to another local state (on the right).

as illustrated in fig. 3. With the local states ordered as indicated in fig. 2, the resultant transfer matrix takes a block-diagonal form

$$T_A = \begin{pmatrix} 1 & 0 & 0 & 0 \\ 0 & 1 & 0 & 0 \\ 0 & 0 & 1 & 0 \\ 0 & 0 & 1 & 1 \end{pmatrix}. \tag{3.4}$$

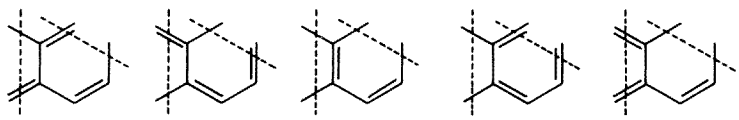

Fig. 4. Manners of "growth" of Kekulé structures across a phenanthrenoid linkage.

For a B-type cell, the five local Kekulé structures of fig. 4 lead to a transfer matrix

$$T_B = \begin{pmatrix} 0 & 1 & 0 & 0 \\ 1 & 0 & 0 & 0 \\ 0 & 0 & 1 & 1 \\ 0 & 0 & 1 & 0 \end{pmatrix} . \tag{3.5}$$

Hence, the resultant ensemble transfer matrix is

$$\mathcal{T} = \begin{pmatrix} x & y & 0 & 0 \\ y & x & 0 & 0 \\ 0 & 0 & x+y & y \\ 0 & 0 & x+y & x \end{pmatrix} . \tag{3.6}$$

Taking powers of this, either algebraically or possibly at given values of x and y, would then allow one to obtain the Kekulé count weighted sum K_L via (3.2).

4. Connection matrices

The conjugated-circuit count quantities $\#^{(m)}$ can be obtained [7] with the use of connection matrices in addition to the transfer matrices. The conjugated circuits around a cycle in any region of the chain may be counted. Consider a region consisting of as few monomer cells as possible, such that the occurrence of a conjugated m-circuit around a chosen m-cycle can be detected solely from a specification of a Kekulé structure within this region. Then let $(\zeta | C_F^{(m)} | \xi)$ denote the number of Kekulé structures, first with a conjugated circuit around the chosen m-cycle and second with local states $|\xi)$ and $|\zeta)$ at the two boundaries of this region consisting of a short sequence of monomer cells identified by the label F. The array $C_F^{(m)}$ is a *connection matrix*. Now, much as in (3.1), the number of Kekulé structures with the considered type of conjugated m-circuit in a basic region consisting of cells j through k is given as

$$\mathrm{tr} \left\{ \left(\prod_i^{<j} T_{C_i} \quad C_F^{(m)} \quad \prod_{\varrho}^{>k} T_{C_\varrho} \right) \right\} . \tag{4.1}$$

Then, an *ensemble connection matrix* may be introduced

$$\mathscr{C}^{(m)} \equiv \sum_F C_F^{(m)} x^{a(F)} y^{b(F)}, \tag{4.2}$$

where $a(F)$ and $b(F)$ are the numbers of A and B monomers in the region F. Then we may evaluate ensemble sums for the considered type of conjugated m-circuits at a given location on the chain as

$$\#_L^{(m)} = L \text{ tr } (\mathscr{C}^{(m)} \mathscr{T}^{L-c(m)}), \quad \text{cyclic chains.} \tag{4.3}$$

In the event, as in sect. 14, that there are different types of conjugated m-circuits with the same value of m but different values of $c(m)$, then there are several corresponding connection matrices $\mathscr{C}^{(m)}$, $\mathscr{C}^{(m)'}$, etc., and $\#_L^{(m)}$ is given as a sum over corresponding terms as on the right-hand side of (4.4).

As an example, consider chains as in fig. 1, with anthracene (A) and phenanthrene (B) linkage. Of the five single-cell structures in fig. 3, only the fourth and possibly the third lead to a conjugated 6-circuit around the 6-cycle, most of which lies within a single cell. The count of occurrences of the conjugated 6-circuit in the fourth structure must equal that where the alternation pattern of single and double bonds around the same cycle is interchanged. Hence, we need count only the first type of circuit (as represented in the fourth structure in fig. 3) and multiply by two to also account for the second type. Thus, we take the only nonzero element of $\mathscr{C}_A^{(6)}$ to be $(11|\mathscr{C}_A^{(6)}|00) = 2$. Likewise, one sees that the fourth structure of fig. 4 leads to our sole nonzero element of the B-matrix, $(11|\mathscr{C}_B^{(6)}|00) = 2$. Then, the ensemble connection matrix for conjugated 6-circuits is

$$\mathscr{C}^{(6)} = \begin{pmatrix} 0 & 0 & 0 & 0 \\ 0 & 0 & 0 & 0 \\ 0 & 0 & 0 & 0 \\ 0 & 0 & 2x+2y & 0 \end{pmatrix}. \tag{4.4}$$

The next smallest size conjugated m-circuits in the present example have $m = 10$ and require $c(m) = 2$ cells. For each pair of types for these two cells, the associated Kekulé structures with a conjugated 10-circuit around the 10-cycle of these two cells are shown in fig. 5. The resultant ensemble connection matrix for conjugated 10-circuits is

$$\mathscr{C}^{(10)} = \begin{pmatrix} 0 & 0 & 0 & 0 \\ 0 & 0 & 0 & 0 \\ 0 & 0 & 0 & 0 \\ 0 & 0 & 2(x+y)^2 & 0 \end{pmatrix}. \tag{4.5}$$

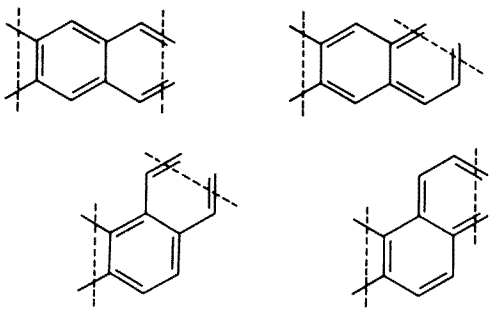

Fig. 5. Different manners of having a conjugated 6-circuit embedded within two monomer cells of the example polyphene system of fig. 1.

In this paper, we neglect conjugated m-circuits with $m \geqslant 12$.

5. Strip ends

The ideas of the preceding two sections are generally extendable to treat the case where boundary conditions other than cyclic are imposed. Sums overs products of transfer matrix elements still yield the desired count much as in (3.1), but with the condition that the initial and final local states may be restricted. If the two ends of the polymer chain are of two fixed forms, the initial and final local states are independently restricted to two corresponding states $|I)$ and $|F)$, respectively, and

$$K_L = (F|\mathcal{T}^L|I) \tag{5.1}$$

in place of (3.2). More generally, a collection of types of ends may be allowed. The general expression is then

$$K_L = \mathrm{tr}\,(\rho\,\mathcal{T}^L), \tag{5.2}$$

where the *end* matrix ρ identifies the type of allowed chain ends and any correlation between these ends. Similarly, the conjugated-circuit count formula of (4.4) extends to

$$\#_L^{(m)} = \sum_{i=0}^{L-c(m)} \mathrm{tr}\,(\rho\,\mathcal{T}^i \mathcal{C}^{(m)} \mathcal{T}^{L-c(m)-i}), \tag{5.3}$$

where the neglected end terms here involve conjugated circuits which impinge upon the local end states. In the limit of long chains ($L \to \infty$), these will be neglected, although if one desired they could be handled by introducing special end correctors

$\rho^{(m)}$. In (5.2) and (5.3), the choice $\rho = \mathbf{1}$ yields (3.2) and (4.4). The choice $\rho = |F)(I|$ in (5.2) yields (5.1). The choice with ρ having the only nonzero elements (= 1) on the "cross diagonal" corresponds to Möbius (twist) boundary conditions.

If the transfer matrix takes a block-diagonal form, different types of ends as specified by ρ may yield quite different predictions. That is, if ρ is nonzero on only one of the blocks of $\mathcal{T}$ (and hence also of C), only properties associated to that block prevail. For the illustrative example of the preceding two sections, just such a block diagonalization applies: property predictions based on the first block are associated to quinoid structures, whereas those based on the second block associate to benzenoid structures. Because of such block-diagonalization there is a type of long-range order, that indeed is a general occurrence and of physical relevance, as is discussed in sect. 9.

6. Eigenanalysis

The transfer- and connection-matrix expressions of the preceding two sections can be refined via eigenanalysis. The ensemble transfer matrix has (at least one pair of) right (r) and left (l) eigenvectors for each eigenvalue λ,

$$\begin{aligned} \mathcal{T}|\lambda, r) &= \lambda|\lambda, r) \\ (\lambda, l|\mathcal{T} &= \lambda(\lambda, l|\,. \end{aligned} \tag{6.1}$$

For each λ corresponding to a 1 by 1 Jordan block, we may biorthonormalize such eigenvectors:

$$(\lambda, l|\lambda', r) = \delta(\lambda, \lambda'). \tag{6.2}$$

If $\mathcal{T}$ is diagonalizable, then the spectral resolution of $\mathcal{T}$ enables (5.2) to be rewritten as

$$K_L = \sum_L (\lambda, l|\rho|\lambda, r)\lambda^L. \tag{6.3}$$

Similarly, the conjugated-circuit enumeration of (5.3) becomes

$$\#_L^{(m)} = \sum_{i=0}^{L-c(m)} \sum_{\lambda,\lambda'} (\lambda, l|\rho|\lambda', r)\,(\lambda')^i (\lambda', l|\mathcal{C}^{(m)}|\lambda, r)\,\lambda^{L-c(m)-i}, \tag{6.4}$$

where here some end corrections are neglected.

The eigensolutions to $\mathcal{T}$ provide a means to make several desired (weighted) enumerations, especially for long chains. For every long chain, it is seen from (6.3) and (6.4) that only the maximum-magnitude eigenvalue(s) come to dominate. Pre-

suming that there is only one such (non-degenerate) eigenvalue Λ which has an associated nonzero matrix element over ρ, we have

$$\begin{aligned} K_L &\to (\Lambda,1|\rho|\Lambda,\mathrm{r})\,\Lambda^L \\ \#_L^{(m)} &\to L(\Lambda,1|\rho|\Lambda,\mathrm{r})\,(\Lambda,1|\mathscr{C}^{(m)}|\Lambda,\mathrm{r})\,\Lambda^{L-c(m)} \end{aligned} \tag{6.5}$$

as $L \to \infty$. Because the quantity K_L involves a (positively weighted) nonzero enumeration when there is at least one Kekulé structure, Λ must be positive real. Since the transfer matrix elements are non-negative, Fröbenius–Perron theory [13] applies, and the eigenvectors associated to the overall maximum-magnitude eigenvalue for a block of $\mathscr{T}$ can be given with all coefficients real and positive on that block (while zero on other blocks). Thus, the condition

$$(\Lambda,1|\rho|\Lambda,\mathrm{r}) \neq 0 \tag{6.6}$$

is realized for the largest eigenvalue of at least one block of $\mathscr{T}$.

As an example, we may continue with the consideration of the type of polymer in fig. 1. From (3.6) one may obtain (right) eigenvectors

$$|x+y) \equiv \frac{1}{\sqrt{2}}\begin{pmatrix}1\\1\end{pmatrix} \quad \text{and} \quad |x-y) \equiv \frac{1}{\sqrt{2}}\begin{pmatrix}1\\-1\end{pmatrix} \tag{6.7}$$

with eigenvalues $x+y$ and $x-y$, respectively, for the first block. Here, the left eigenvectors are obtained by transposing. For the second block, the left and right eigenvectors are less trivially related

$$\begin{aligned} |\lambda,\mathrm{r}) &= \begin{pmatrix}-y\\ x+y-\lambda\end{pmatrix} \\ (\lambda,1| &= \{y(x-\lambda)+(x+y-\lambda)y\}^{-1}\,(\lambda-x \quad y) \end{aligned} \tag{6.8}$$

for the eigenvalues

$$\lambda = x + \frac{y}{2} \pm \sqrt{xy+\tfrac{5}{4}y^2} \tag{6.9}$$

as are all well-defined for $x \geqslant 0$, $y > 0$. For the remaining special singular case of $y = 0$, the whole second block of $\mathscr{T}$ identifies a single Jordan block whose single right eigenvector is the last basis vector, and whose eigenvalue is x.

7. Long-chain limit

For the large sysem limit, "bulk" properties often exhibit an independence of the ensemble chosen for making the calculation. A first step toward the elucidation of this feature concerns the nature of the $L \to \infty$ asymptotic forms for the Kekulé structure counts

$$K_L \to C \Lambda^L \tag{7.1}$$

and

$$K_{a,b} \to C_\alpha L^\xi \Lambda_\alpha^L , \tag{7.2}$$

where $L \equiv a + b$ is the chain length and $\alpha \equiv a/L$. The first of these relations (7.1) follows immediately from (6.4) for the case where $\mathcal{T}$ has its maximum eigenvalue in a trivial (i.e. 1 by 1) Jordan block. The second form (7.2) is a more delicate matter and may occur only in a *locally averaged* way. The form of (7.2) can in principle be obtained from a knowledge of K_L if we note that $\binom{a+b}{a} K_{a,b}$ is simply the coefficient of $x^a y^{L-a}$ in $K_L(x, y)$. Then, from the Cauchy relation

$$\binom{L}{a} K_{a,b} = \frac{1}{2\pi i} \oint K_L(z, 1) \frac{1}{z^{a+1}} \, dz, \tag{7.3}$$

with the integration contour around the origin enclosing no singularity of $K_L(z, 1)$. As a consequence, the $K_{a,b}$ consistent with K_L is unique. Hence, we merely seek to show that the form (7.2) leads to (7.1).

We expand K_L in terms of the $K_{a,b}$

$$K_L = \sum_a \binom{L}{a} K_{a,L-a} x^a y^{L-a} \cong \sum_a L^\xi \binom{L}{\alpha L} C_\alpha \Lambda^L x^{\alpha L} y^{(1-\alpha)L}. \tag{7.4}$$

With the presumption that Λ_α (and C_α) vary sufficiently gradually with α, as may require local averaging, the sum here may be approximated as an integration over α. Further, utilizing Stirling's formula for the factorials, we obtain

$$K_L \cong \frac{L^{\xi + 1/2}}{\sqrt{2\pi}} \int_0^1 \frac{C_\alpha}{\sqrt{\alpha(1-\alpha)}} \left\{ \Lambda_\alpha \left(\frac{x}{\alpha}\right)^\alpha \left(\frac{1-x}{1-\alpha}\right)^{1-\alpha} \right\}^L dx . \tag{7.5}$$

For the limit of large lengths L, the α values making the dominant contribution to the integral are those near the maximum of the factor raised to the Lth power. Hence,

we approximate this factor near its maximum at $\alpha = \bar{\alpha}$, for which we assume $0 < \bar{\alpha} < 1$, so that [14]

$$f(\alpha) \equiv \Lambda_\alpha \left(\frac{x}{\alpha}\right)^\alpha \left(\frac{1-x}{1-\alpha}\right)^{1-\alpha} \cong f(\bar{\alpha})\{1 - \kappa(\alpha - \bar{\alpha})^2\}, \tag{7.6}$$

where κ is a "scaled" second derivative with respect to α, at $\alpha = \bar{\alpha}$. Then

$$K_L \cong \frac{L^{\xi+1/2}}{\sqrt{2\pi}} \frac{C_{\bar{\alpha}}}{\bar{\alpha}(1-\bar{\alpha})} \{f(\bar{\alpha})\}^L \int_0^1 e^{-\kappa(\alpha-\bar{\alpha})^2 L} d\alpha . \tag{7.7}$$

However, by introducing a new variable $u \equiv (\alpha - \bar{\alpha})\sqrt{\kappa L}$, one may evaluate the remaining integral for the limit $L \to \infty$. We find

$$K_L \cong \frac{C_{\bar{\alpha}}}{\sqrt{2\kappa\bar{\alpha}(1-\bar{\alpha})}} L\{f(\bar{\alpha})\}^L, \tag{7.8}$$

Evidently, this conforms with the established asymptotic form of (7.1), and

$$\begin{aligned} \Lambda &= \Lambda_{\bar{\alpha}} \left(\frac{x}{\bar{\alpha}}\right)^{\bar{\alpha}} \left(\frac{1-x}{1-\bar{\alpha}}\right)^{1-\bar{\alpha}} \\ C &= C_{\bar{\alpha}}\{2\kappa\bar{\alpha}(1-\bar{\alpha})\}^{-1/2} \\ \xi &= 0. \end{aligned} \tag{7.9}$$

If the maximum $\bar{\alpha}$ lies instead at the end points of integration, $\bar{\alpha} = 0$ or 1, then the arguments and formulae of (7.9) are modified, in particular then $\xi = +1/2$.

8. Long-chain expectation values

Computational convenience is achieved if the contribution of conjugated m-circuits to an ensemble-average energy per site in long chains may be argued to be given in terms of

$$\epsilon^{(m)} = \lim_{L \to \infty} \#_L^{(m)}/LK_L . \tag{8.1}$$

It is to be emphasized that these $\#_L^{(m)}$ values generally differ (at the same value of x and y) from what might be identified as the physically relevant averages

$$\hat{\epsilon}^{(m)} = \lim_{L \to \infty} \frac{1}{L} \sum_{G} x^{a(G)} y^{b(G)} \epsilon^{(m)}(G), \tag{8.2}$$

where

$$\epsilon^{(m)}(G) = \frac{\#^{(m)}(G)}{LK(G)} . \tag{8.3}$$

That is, the ratio of the averages as in (8.1) generally differs from the average of the ratios as in (8.2).

Nevertheless (at least for chain length $L \to \infty$), we conjecture a simple relationship. This relationship is to be discerned in terms of a hypothesized "normalized" distribution $\rho_L(\alpha)$. That is, $\binom{L}{\alpha L}\rho_L(\alpha)\mathrm{d}\alpha$ is to be the number of length-L systems, with a/L taking a value between α and $\alpha + \mathrm{d}\alpha$. The binomial coefficient (having to do with the different ways of distributing αL A-monomers amongst L positions) is to separate out the rapidly varying part of the overall distribution. It is presumed, as in indicated in the previous section, that $\rho_L(\alpha)$ varies with L at most as a (bounded) power of L. Then, as is implied from sect. 7,

$$K_L = \int_0^1 K_\alpha \rho_L(\alpha) \binom{L}{\alpha L} \{x^\alpha (1-x)^{1-\alpha}\}^L \mathrm{d}\alpha$$

$$\#_L^{(m)} = \int_0^1 \#_\alpha^{(m)} \rho_L(\alpha) \binom{L}{\alpha L} \{x^\alpha (1-x)^{1-\alpha}\}^L \mathrm{d}\alpha, \tag{8.4}$$

with the integrals dominated by α values near the $\bar{\alpha}$ value identified in terms of Λ_α following eq. (7.5). However, now also

$$\hat{\epsilon}_L^{(m)} = \int_0^1 \epsilon_\alpha^{(m)} \rho_L(\alpha) \binom{L}{\alpha L} \{x^\alpha (1-x)^{1-\alpha}\} \mathrm{d}\alpha, \tag{8.5}$$

with the dominating α values not determined in terms of Λ_α. Rather, they are similarly seen to be near $\alpha = \hat{x}$, which is at the maximum of $x^\alpha (1-x)^{1-\alpha} \binom{L}{\alpha L}^{1/L}$. Thus, at the same value of x (and $y = 1 - x$), we see that α and x are generally different and so also are $\epsilon^{(m)}$ and $\hat{\epsilon}^{(m)}$ of (8.1) and (8.2). Suppose instead that we compare $\epsilon^{(m)}$ and $\hat{\epsilon}^{(m)}$ at different values of x. Indeed, suppose x is replaced by $\hat{x}$ in the second expression with $\hat{x} = \bar{\alpha}$. Because the Lth powers (including a factor arising from the binomial coefficient) involved in the integrals of (8.4) sample mainly systems with α values near

the average, we then expect the same system to be sampled so that $\epsilon^{(m)} = \hat{\epsilon}^{(m)}$. More explicitly, indicating the x- or $\hat{x}$-dependence, we write

$$\epsilon^{(m)}(x) = \hat{\epsilon}^{(m)}(\bar{\alpha}), \tag{8.6}$$

which is the desired relation.

A final point concerns computationally amenable expressions for $\epsilon^{(m)}$ and $\bar{\alpha}$. First, from (6.4) one obtains

$$\epsilon^{(m)} = (\lambda, 1|\mathcal{C}^{(m)}|\Lambda, r)/\Lambda^{c(m)} . \tag{8.7}$$

Via a parallel development,

$$\bar{\alpha} = \lim_{L\to\infty}\left[\frac{1}{LK_L}\frac{\partial K_L(x,y)}{\partial \ln x}\right] = \frac{1}{\Lambda}\frac{\partial \Lambda}{\partial \ln x}, \quad \text{at } x+y=1, \tag{8.8}$$

where we have utilized (5.1), (3.3) and (6.4). Now, with the use of the Hellman–Feynman theorem (or first-order perturbation theory), one obtains

$$\bar{\alpha} = x(\Lambda, 1|T_A|\Lambda, r)/\Lambda . \tag{8.9}$$

The overall ensembe-average energy per monomer

$$\epsilon = \sum_{p\geq 1}\left\{R_p\,\epsilon^{(4p+2)} + Q_p\,\epsilon^{(4p)}\right\} \tag{8.10}$$

has parameters as in (2.1). Here, $\epsilon^{(m)}$ and ϵ are viewed as functions of $\bar{\alpha}$ or (in abbreviated form) just α, with (8.7), (8.9) and (8.10) being the desired computationally amenable expressions.

9. Long-range spin-pairing order

Generally, it may be shown that there is some blocking (e.g. block diagonalization) of the transfer and connection matrices. First, for a local state $|\xi)$ with π-bond occupation numbers $\xi_1, \ldots, \xi_w = 0$ or 1 on the w different interconnections between monomer units, we assign a *resonance-parity quantum number,* defined as

$$q_\xi \equiv \begin{cases} -, & \sum_{i=1}^{w}\xi_i = \text{odd} \\ +, & \sum_{i=1}^{w}\xi_i = \text{even} . \end{cases} \tag{9.1}$$

Next, in any Kekulé structure, each double bond completely within a unit cell accounts for two of the $n(C)$ sites in a monomer cell of type C, while each double bond crossing a cell boundary (and appearing in one of the two associated local states) utilizes but one site in the cell. Thus, for a cell bounded by local states $|\xi)$ and $|\zeta)$, the quantity

$$n(C) - \sum_{i=1}^{w} \xi_i - \sum_{i=1}^{w} \zeta_i \tag{9.2}$$

is just twice the number of double bonds entirely within the cell. Therefore, the parity of (9.2) must be even and

$$(\zeta | T_C | \xi) = 0, \quad \text{if} \quad q_\xi = -(-1)^{n(C)} q_\zeta \,. \tag{9.3}$$

Hence, T_C is blocked with regard to resonance parity quantum numbers; this blocking is either block- or cross-block-diagonal as $n(C)$ is even or odd, respectively. Similar blocking applies to the corresponding connection matrices.

In the example with anthracene- and phenanthrene-like fusions, two 2×2 diagonal blocks are readily discernable in (3.6), (4.4) and (4.5). The first and second blocks correspond to the spaces with bases $|01), |10)$ and $|00), |11)$, respectively.

The resonance parity quantum number and associated blocking has physicochemical consequences, which we consider here for the case where all $n(C)$ are even. This entails a type of *long-range spin-pairing order* [3,6,15] where the resonance parity of each local state down a polymer chain is the same. In this case, the two blocks ($q = +$ and $-$) may be treated separately to yield two different energies

$$\epsilon^q = \sum_{p \geq 1} (R_p \epsilon^{(2p+2)q} + Q_p \epsilon^{(2p)q}), \tag{9.4}$$

where $\epsilon^{(m)q}$ is computed only from the $q = +$ and $q = -$ blocks. That is, they are computed in the case where one views the choice of ends, as embodied in ρ, to be made so that the ρ is simply a projection onto one or the other block space. Denoting the largest eigenvalue of block q by Λ_q, we have

$$K_L^q \to C^q \Lambda_q^L$$

$$\#_L^{(m)q} \to C^q L \epsilon^{(m)q} \Lambda_q^L \,, \tag{9.5}$$

where

$$C^q = (\Lambda_q, 1|\rho_q|\Lambda_q, r)$$
$$\epsilon^{(m)q} = (\Lambda_q, 1|\mathscr{C}^{(m)}|\Lambda_q, r) \tag{9.6}$$

so that the two quite different energies occur. Thus, the more stable energy ϵ^q can change abruptly from one value of q to another with a gradual change in system parameter, such as the fraction α of the system which is of type A monomers. Moreover, the asymptotic result so obtained would be the same as that obtained with cyclic boundary conditions only when the largest Λ_q corresponds with the lowest ϵ^q. Of course, this correspondence is viewed in resonance theory [16] to apply approximately, at least for benzenoids. Generally, however, this would lead to a non-physical discontinuous jump in the system energy. The correct physico-chemical choice (as $L \to \infty$) is just the lower of the two ϵ^q, a jump from one to the other typically identifying a "first-order" transition, here occurring as a function of α at zero temperature. Moreover, at such a crossing there is generally a discontinuous change in the patterns of bond localization, i.e. the bond lengths in A and B cells change abruptly. Yet further, the consequent degeneracy of $q = +$ and $q = -$ phases at the crossing leads to the possibility of a novel type of solitonic excitation [2–4,7].

10. Overall computational scheme

At this point, a systematic overall computational scheme for long chains has emerged. For given monomer units A and B, we follow a sequence of steps:

(1) Determine T_A, T_B, $\mathscr{C}_A^{(m)}$, $\mathscr{C}_B^{(m)}$, for $m \leqslant 10$.
(2) For a choice of x and $y = 1 - x$, determine $\mathscr{T}$ via (3.3) and $\mathscr{C}^{(m)}$ via (4.2).
(3) Find the maximum eigenvalue Λ in each block of $\mathscr{T}$ and determine the associated eigenvectors.
(4) Determine $\epsilon^{(m)}$, $\bar{\alpha}$, and ϵ associated to each block of $\mathscr{T}$ using (8.7), (8.9) and (8.10).

Here, Λ is a Kekulé count (per monomer), while ϵ (and $\log \Lambda$) is an energy estimate. Each of Λ, $\epsilon^{(m)}$, and ϵ is viewed as a function of α, the fraction of A monomers, which may be varied (from 0 to 1) by varying the choice of x from 0 to 1. Finally, from ϵ^q versus α curves for different long-range order parameters (e.g. parities q), various physico-chemical consequences (e.g. zero temperature phase transitions) may be deduced via considerations as in sect. 9.

11. Catacondensed polyphene chains

With the concepts and methods from the preceding sections set in place, we now investigate several simple systems, the first of which is the system of fig. 1 used

as an illustrative example in much of the preceding. The maximum eigenvalues of the first ($q = -$) and second ($q = +$) blocks of $\mathcal{T}$ are seen from the results at the end of sect. 6 to become

$$\begin{aligned} \Lambda_- &= 1 \\ \Lambda_+ &= \{1 + x + \sqrt{(1-x)(5-x)}\}/2 \end{aligned} \tag{11.1}$$

when the "activity-normalization" of (2.4) is imposed. Then the asymptotic counts become, with some use of (4.4) and (4.5),

$$\begin{aligned} K_L^- &\to C^- \\ K_L^+ &\to C^+ \Lambda_+^L \\ \#_L^{(m)-} &\to 0 \\ \#_L^{(m)+} &\to C^+ L\, \epsilon^{(m)+} \Lambda_+^L , \end{aligned} \tag{11.2}$$

where $\#_L^{(m)}$ (or, more basically, $\epsilon^{(m)-}$) is realized only to approach 0 in the sense that whatever terms do occur are not size-extensive (being associated to the ends only). Next, utilizing (8.7) and the eigenvectors of sect. 6, we have

$$\begin{aligned} \epsilon^{(2m)-} &= \epsilon^{(8)+} = 0 \\ \epsilon^{(6)+} &= \epsilon^{(10)+} = 2\sqrt{(1-x)/(5-x)} \ . \end{aligned} \tag{11.3}$$

As a consequence our estimate of the overall π-resonance energy per site is

$$\begin{aligned} \epsilon^- &= 0 \\ \epsilon^+ &= 2(R_1 + R_2)\sqrt{(1-x)/(5-x)} \, . \end{aligned} \tag{11.4}$$

The corresponding fraction of A monomers is computable, via (8.9) and (11.1), to yield

$$\begin{aligned} \alpha^- &= x \\ \alpha^+ &= x\{1 + \sqrt{(1-x)/(5-x)}\}/\Lambda_+ , \end{aligned} \tag{11.5}$$

where again we have taken $x + y = 1$. A plot of the resultant ensemble-average energy as a function of A-monomer fraction α is shown in fig. 6.

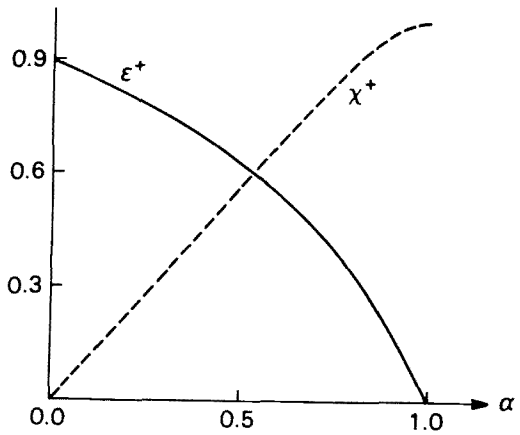

Fig. 6. The resonance energy per monomer (solid line) and the activity (dashed line) of the preferred $q = +$ phase of the random polyphenes of sect. 11 as a function of the fraction α of anthracenoid linkages.

12. p-phenyl-α-napthyl chains

This example involves the two monomer units of fig. 7. These can be connected together in random sequences, as in fig. 8. Since there is but a single connection between each cell, the possible local states are:

$$|0) \quad \text{and} \quad |1). \tag{12.1}$$

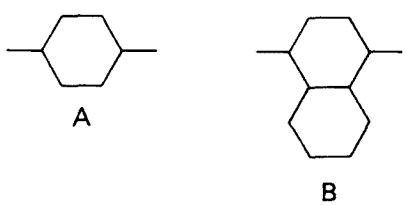

Fig. 7. Monomer cells for the random polymer of sect. 12.

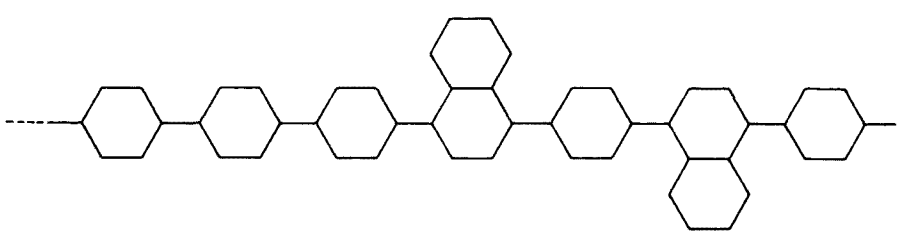

Fig. 8. A portion of a random polymer of the type discussed in sect. 12.

Moreover, since the first is identified to a resonance quantum number of $q = +$ and the second to one of $q = -$, the transfer and connection matrices turn out to be (block) diagonal. The relevant matrices for a benzene cell are readily found to be:

$$T_A = \begin{pmatrix} 2 & 0 \\ 0 & 1 \end{pmatrix}, \quad C_A^{(6)} = \begin{pmatrix} 2 & 0 \\ 0 & 0 \end{pmatrix}, \quad C_A^{(10)} = \begin{pmatrix} 0 & 0 \\ 0 & 0 \end{pmatrix}, \tag{12.2}$$

where, for instance, the first element of T_A indicates that there are two Kekulé structures if the incoming and outgoing bonds are single. That the off-diagonal elements are 0 indicates there are no Kekulé structures when one of the joining bonds is single and the other double. For a napthalene cell, one similarly obtains

$$T_B = \begin{pmatrix} 3 & 0 \\ 0 & 2 \end{pmatrix}, \quad C_B^{(6)} = \begin{pmatrix} 4 & 0 \\ 0 & 2 \end{pmatrix}, \quad C_B^{(10)} = \begin{pmatrix} 2 & 0 \\ 0 & 0 \end{pmatrix}. \tag{12.3}$$

Then, the ensemble matrices are

$$\mathcal{T} = \begin{pmatrix} 2x + 3y & 0 \\ 0 & x + 2y \end{pmatrix}, \mathcal{C}^{(6)} = \begin{pmatrix} 2x + 4y & 0 \\ 0 & 2y \end{pmatrix}, \mathcal{C}^{(10)} = \begin{pmatrix} 2y & 0 \\ 0 & 0 \end{pmatrix}. \tag{12.4}$$

The eigenvalues are of course just the diagonal elements of $\mathcal{T}$ and the eigenstates are the basis vectors of (12.1). Clearly

$$\begin{aligned} \alpha^+ &= \frac{2x}{2x + 3y} = \frac{2x}{3 - x} \\ \alpha^- &= \frac{x}{x + 2y} = \frac{x}{2 - x}, \end{aligned} \tag{12.5}$$

where we have used $x + y = 1$. Similarly, the resonance energies are

$$\begin{aligned} \epsilon^+ &= \frac{4 - 2x}{3 - x} R_1 + \frac{2 - 2x}{3 - x} R_2 \\ &= \tfrac{1}{3}\{4 - \alpha\}R_1 + \tfrac{2}{3}\{1 - \alpha\}R_2 \\ \epsilon^- &= \frac{2 - 2x}{2 - x} R_1 = \{1 - \alpha\}R_1. \end{aligned} \tag{12.6}$$

For any parameterization with $R_1 > 0$ and $R_2 \geqslant 0$, it may be seen that the $q = +$ phase is more stable for all α, and thus describes the ground state.

13. Anthryl-α-napthyl chains

The next example system consists of the two singly-connected monomer units of fig. 9. The local states are again as in (12.1), and the treatment is rather similar to that of sect. 12. The present resultant ensemble matrices are

$$\mathcal{T} = \begin{pmatrix} 4x + 3y & 0 \\ 0 & 4x + 2y \end{pmatrix}, \quad \mathcal{C}^{(6)} = \begin{pmatrix} 6x + 4y & 0 \\ 0 & 8x + 2y \end{pmatrix}, \quad \mathcal{C}^{(10)} = \begin{pmatrix} 4x + 2y & 0 \\ 0 & 0 \end{pmatrix}. \tag{13.1}$$

The fractions of A cells are

$$\bar{\alpha}^{+} = \frac{4x}{4x + 3y} = \frac{4x}{3 + x}$$

$$\bar{\alpha}^{-} = \frac{4x}{4x + 2y} = \frac{2x}{1 + x}, \tag{13.2}$$

and the resonance energies per cell are

$$\epsilon^{+} = \frac{6x + 4y}{4x + 3y} R_1 + \frac{4x + 2y}{4x + 3y} R_2$$

$$= (\tfrac{4}{3} R_1 + \tfrac{2}{3} R_2) + (\tfrac{1}{6} R_1 + \tfrac{1}{3} R_2)\bar{\alpha}^{+} \tag{13.3}$$

$$\epsilon^{-} = \frac{8x + 2y}{4x + 2y} R_1 = R_1 + R_1 \bar{\alpha}^{-}.$$

With parameters [10]

$$R_1 = 0.841 \text{ eV} \quad \text{and} \quad R_2 = 0.336 \text{ eV}, \tag{13.4}$$

we obtain a plot of these energies as a function of $\alpha = \bar{\alpha}^{+} = \bar{\alpha}^{-}$, as in fig. 10. It is seen that with increasing α, there is a (zero-temperature phase) transition from $q = -$ to $q = +$ at $\alpha \cong \frac{2}{3}$. Here, the joining bonds between monomer units changes abruptly from single to double. Further, precisely at the transition point where there is phase degeneracy, solitonic excitations [2,4,7] can arise.

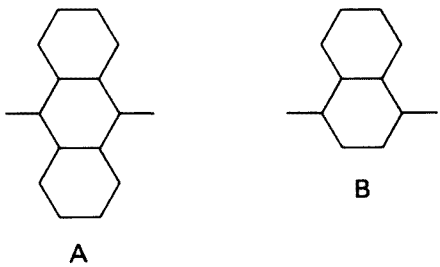

Fig. 9. Monomer cells for the random polymer of sect. 13.

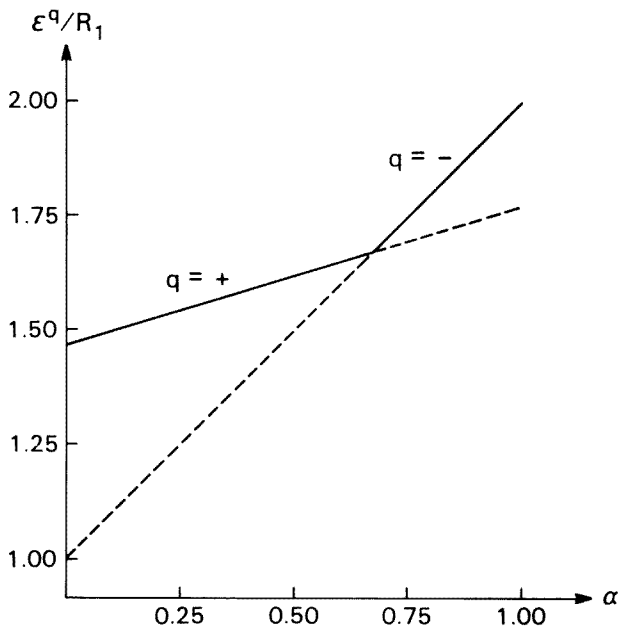

Fig. 10. The q = + and q = − resonance energies per monomer for random polymers of the type in sect. 13 as a function of the fraction α of anthracene monomers (A).

14. Polynapthalenoid chains

Recently, the polymeric species with unit cells of type A in fig. 11 has [17] been synthesized and found to be rather conductive. In another synthetic approach [18], an excess of hydrogen remains, perhaps due to unit cells of type B or B' in the figure. There are eight imaginable ways to occupy the three boundary bonds on one side of a monomer cell. However, |000) does not occur for any Kekulé structure, and |111) does not occur for any involving a B or B' cell anywhere along the polymer chain. Hence, there remain two different parity spaces with local-state bases

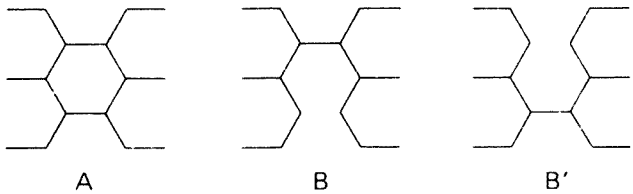

Fig. 11. The three types of 6-site monomer cells for the random polymers considered in sect. 14.

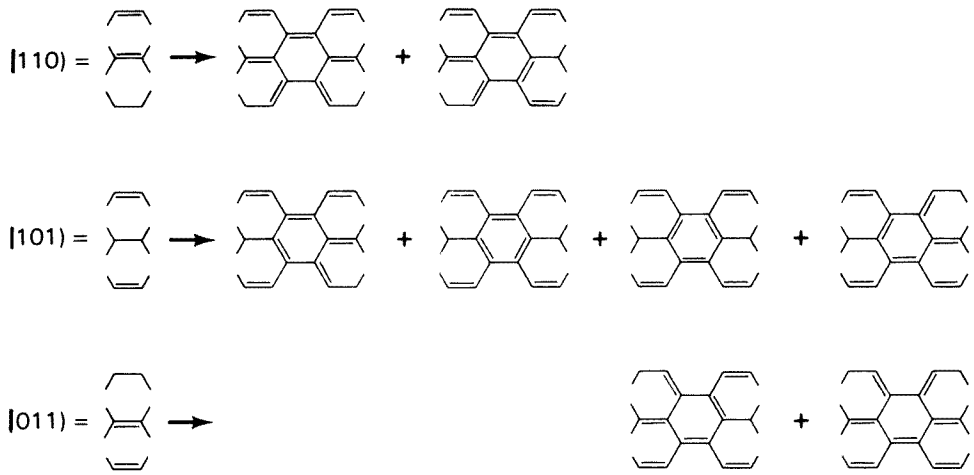

Fig. 12. Manner of propagation of $q = +$ Kekulé structures across an A-type monomer cell.

$$\begin{aligned} &|100), |010), |001) \ , q = - \\ &|110), |101), |011) \ , q = + . \end{aligned} \tag{14.1}$$

The odd- and even-parity blocks for an A cell are

$$T_A^+ = \begin{pmatrix} 1 & 1 & 0 \\ 1 & 2 & 1 \\ 0 & 1 & 1 \end{pmatrix}, \qquad T_A^- = \begin{pmatrix} 1 & 1 & 1 \\ 1 & 1 & 1 \\ 1 & 1 & 1 \end{pmatrix}, \tag{14.2}$$

where, for instance, the diagrammatic derivaton of the $q = +$ block is outlined in fig. 12. For the B-type cells, we presume that the B and B' cells (of fig. 11) occur with equal likelihood, so that in place of T_B in the ensemble matrix $\mathcal{T}$ we simply insert the average of transfer matrices for B and B'. We denote this average simply by T_B,

and find its $q = +$ block to be half of T_A^+ and its $q = -$ block to be the same as T_A^-. As a consequence

$$\mathcal{T}^+ = (x + y/2)\,T_A^+$$
$$\mathcal{T}^- = (x + y)\,T_A^- . \tag{14.3}$$

Now the maximum eigenvalues to the $\mathcal{T}^q$ are found to be $\Lambda^+ = 3(x + y/2)$ and $\Lambda^- = 3(x + y)$. At this point, within the Kekulé count approximation [16] for estimating resonance energies, one obtains two ($q = +$ and $q = -$) degernate phases only at a single point $\alpha = x = 1$. This marginal circumstance can quite possibly be expected to be modified in a qualitative way with better energy estimates.

For the conjugated-circuit connection matrices, care needs to be taken since generally there are two ways of realizing relevant cycles as occurring within one ($c(m) = 1$) or two ($c(m) = 2$) monomer cells. In particular, this circumstance applies for 6-cycles occurring in A cells, as indicated in fig. 13. Hence, we find

$$\mathcal{C}^{(6)'+} = \begin{pmatrix} 0 & 0 & 0 \\ 0 & 2x & 0 \\ 0 & 0 & 0 \end{pmatrix}, \quad \mathcal{C}^{(6)'-} = \mathbf{0} \tag{14.4}$$

for that cycle (with $c(6) = 1$) identified by a "1" in fig. 13, and

$$\mathcal{C}^{(6)+} = \left(x + \frac{y}{2}\right)^2 \begin{pmatrix} 2 & 2 & 2 \\ 2 & 4 & 2 \\ 0 & 2 & 2 \end{pmatrix}, \quad \mathcal{C}^{(6)-} = (x + y)^2 \begin{pmatrix} 4 & 4 & 4 \\ 4 & 4 & 4 \\ 4 & 4 & 4 \end{pmatrix} \tag{14.5}$$

for the cycles (with $c(6) = 2$) identified by a "2" in fig. 13. The various possible conjugated 10-circuits all span two monomer cells and yield

$$\mathcal{C}^{(10)+} = \left(x^2 + \frac{xy}{2}\right) \begin{pmatrix} 0 & 2 & 0 \\ 2 & 8 & 2 \\ 0 & 2 & 0 \end{pmatrix}, \quad \mathcal{C}^{(10)-} = (x + y)^2 \begin{pmatrix} 2 & 2 & 2 \\ 2 & 2 & 2 \\ 2 & 2 & 2 \end{pmatrix}. \tag{14.6}$$

The solution proceeds with the evaluation of matrix elements over the maximum-eigenvalue eigenvector.

The solution to the present problem is completed following the outline of sect. 10. The resultant resonance energies for the $q = +$ and $q = -$ phases are

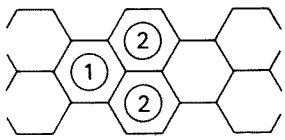

Fig. 13. Identification of the different types of 6-cycles in a pair of A-monomer cells, as considered in the text.

$$\epsilon^{+} = (\tfrac{4}{9}\alpha + \tfrac{2}{3})R_1 + \tfrac{8}{9}\alpha R_2$$
$$\epsilon^{-} = \tfrac{16}{9}R_1 + \tfrac{8}{9}R_2 \,. \tag{14.7}$$

For all (reasonable) parameterizations with $R_1 > R_2 > 0$ at all α, this yields the $q = -$ phase as the sole stable phase (even, quite notably, at $\alpha = x = 1$). As a consequence, this material should smoothly change with variations in α, and there should be no solitonic excitations. Should material containing other types of impurities (defects), or should a different type of ensemble apply for the realized polymer growth process, the conclusions reached could in principle be different. However, since the $q = -$ phase is presently quite stable (by $\geqslant 2R_1/3$ at all α with the parameterization of (13.4)), a rather strong perturbation would be required to make a qualitative change so that the $q = +$ phase is preferred (at some α).

15. Conclusions

Resonance-theoretic ideas have been developed for ensembles of random polymers. A choice was made to study ensembles with a single activity (or weight) for each type of monomer unit. Secondly, a choice was made to focus on the conjugated-circuit model for such random polymers. Then, an efficient transfer-matrix method was developed for this application, the practical computational implementation of which is summarized in sect. 10. Following this, the method was illustrated for a few simple systems. The possibilities of "degenerate" phases, solitonic excitations, and phase transitions (as a function of monomer concentrations) have been noted. The transfer-matrix technique and these novel physical consequences should still apply under somewhat more general circumstances, including: first, the extension of the ensemble averaging to allow nearest-neighbor pair activities; second, the extension to allow more than two types of monomer units; third, the application to other than (alternant) benzenoids; and fourth, the utilization of alternative types of resonance-theoretic models, such as that by Pauling and Wheland.

References

[1] See, for example:
(a) H.A. Pohl, J. Polym. Sci. C17(1967)13.
(b) A. Rembaum, J. Polym. Sci. C29(1970)157.
(c) A.A. Ovchinnikov and I.A. Misurkin, Russ. Chem. Rev. (Engl. trans.) 46(1977)967.
(d) A. Graovac, I. Gutman, M. Randić and N. Trinajstić, Colloid & Polymer Sci. 225(1977) 480.
(e) C.B. Duke and H.W. Gibson, in: Kirk-Othmer: *Encyclopedia of Chemical Technology,* Vol. 18 (Wiley, New York, 1982) pp. 755–795.
(f) *Proc. Physique et la Chimie des Polymères Conducteurs,* Les Arcs (1983), ed. R. Comes, P. Bernier, J.J. Andre and J. Rouxel, J. de Phys. 44-C3 (1983).

[2] (a) W.P. Su, J.R. Schrieffer and A.J. Heeger, Phys. Rev. Lett. 42(1979)1698.
(b) M.J. Rice, Phys. Lett. 71A(1979)152.
(c) A.J. Heeger, Comments in Solid State Physics 10(1981)53.
(d) D.S. Boudreaux, R.R. Chance, R.L. Elsenbaumer, J.E. Frommer and R. Silbey, Phys. Rev. B31(1985)652.
(e) *Proc. Conf. on Synthetic Metals II,* Los Alamos (1983), ed. R. Liepins and S. Mazumdar, Synth. Metals 9, No. 2 (1984).

[3] F.L. Carter, Physica 10D(1984)175.

[4] D.J. Klein, T.G. Schmalz, W.A. Seitz and G.E. Hite, Int. J. Quantum Chem. 195(1986)707.

[5] See, for example, P.J. Flory, *Polymer Chemistry* (Cornell University Press, Ithaca, New York, 1953) Ch. V.

[6] See, for example:
(a) E.H. Lieb and D.C. Mattis, *Mathematical Physics in One Dimension* (Academic Press, New York, 1966) Ch. 3.
(b) J. Hori, *Spectral Properties of Disordered Chains and Lattices* (Pergamon, London, 1968).
(c) J.M. Ziman, *Models of Disorder* (Cambridge University Press, Cambridge, 1979) Chs. 2 and 8.

[7] (a) D.J. Klein, T.G. Schmalz, G.E. Hite, A. Metropoulos and W.A. Seitz, Chem. Phys. Lett. 120(1985)367.
(b) G.E. Hite, A. Metropoulos, D.J. Klein, T.G. Schmalz and W.A. Seitz, Theor. Chim. Acta 69(1986)369.

[8] D.J. Klein, G.E. Hite and T.G. Schmalz, J. Comp. Chem. 7(1986)443.

[9] (a) M. Randić, Chem. Phys. Lett.
(b) M. Randić, Tetrahedron 33(1977)1906.

[10] (a) W.C. Herndon, J. Amer. Chem. Soc. 95(1973)2404.
(b) W.C. Herndon and M.L. Ellzey, Jr., J. Amer. Chem. Soc. 96(1974)6631.

[11] (a) I. Gutman and W.C. Herndon, Chem. Phys. Lett. 34(1975)387.
(b) W.C. Herndon, Isr. J. Chem. 20(1980)270.

[12] For application to related graph-theoretic enumeration problems, see, for example,
(a) D.J. Klein, J. Stat. Phys. 23(1980)561.
(b) B. Derrida, J. Phys. A14(1981)L5.
(c) J.P. Nadal, B. Derrida and J. Vannimenus, J. de Phys. 43(1982)1561.
(d) A. Graovac, O.E. Polansky and N.N. Tyutyulkov, Croat. Chim. Acta 56(1983)315.

[13] See, for example, F.R. Gantmacher, *The Theory of Matrices,* Vol. II (Chelsea, New York, 1959) Ch. 13.

[14] The asymptotic integral evaluation method used here is the standard "steepest descent" technique of statistical mechanics.

[15] (a) D.J. Klein and M.A. García-Bach, Phys. Rev. B19(1979)877.
(b) D.J. Klein, Int. J. Quantum Chem. 13S(1979)293.
[16] (a) P.G. Carter, Trans. Faraday Soc. 45(1949)497.
(b) R. Swinbourne-Sheldrake, W.C. Herndon and I. Gutman, Tetrahedron Lett. 1975(1975) 755.
[17] M. Murakami and S. Yoshimura, Chem. Soc., Chem. Comm. (1984) 1649; Mol. Cryst. Liq. Cryst. 118(1985)95.
[18] W.C. Herndon, private communication.